Tribol Lett (2011) 43:329–339
DOI 10.1007/s11249-011-9814-6

ORIGINAL PAPER

Achieving Low Tribological Moisture Sensitivity by a-C:Si:Al Carbon-based Coating

Shengguo Zhou · Liping Wang · Qunji Xue

Received: 10 March 2011 / Accepted: 11 June 2011 / Published online: 24 June 2011

Abstract Owing to the requirements of the stable operation for mechanical components, the urgent challenges are to control tribological moisture sensitivity of protective coatings. In this letter, a-C:Si and a-C:Si:Al carbon-based coatings were successfully fabricated via magnetron sputtering Si, Al, and C. The microstructure, mechanical properties, and tribological moisture sensitivity of as-fabricated carbon-based coatings were comparatively investigated. Results showed that the as-fabricated a-C:Si and a-C:Si:Al coatings were dominated by typical amorphous structure. The co-introduction of Al could effectively relax internal stress and improve adhesive strength as well as maintain the moderately high hardness for the as-fabricated coating. The striking improvement in tribological moisture sensitivity of a-C:Si:Al carbon-based coating was mainly attributed to the superior mechanical properties and the formation of continuously compacted graphitized tribofilm under low relative humidity condition as well as low shear strength colloidal silica tribofilm under high relative humidity condition. The good balance between the hardness and toughness, low internal stress, and superior low tribological moisture sensitivity of a-C:Si:Al coating make it a good candidate for solid lubricating coating in engineering applications.

S. Zhou · L. Wang (✉) · Q. Xue
State Key Laboratory of Solid Lubrication, Lanzhou Institute of Chemical Physics, Chinese Academy of Sciences, Lanzhou 730000, People's Republic of China
e-mail: lpwang@licp.cas.cn

S. Zhou
Graduate University of Chinese Academy of Sciences, Beijing 100039, People's Republic of China

Keywords Internal stress · a-C:Si:Al · Tribofilm · Moisture sensitivity

1 Introduction

The carbon-based coatings characterized by high hardness, low internal stress, good toughness, and low tribological moisture sensitivity are of continuously increased significance in the engineering applications [1–6]. Unfortunately, successful applications of carbon-based coatings have been considerably restricted by the high internal stress and poor adhesion to some substrates, especially, they could increase friction coefficient and quickly fail in high humid or aqueous environments [7–12]. Therefore, many researchers have devoted to the preparation of carbon-based coatings by doping additional elements to overcome those drawbacks. Among those studies, silicon incorporation in the carbon-based coatings has been widely studied and was reported as being effective in improving tribological performances in ambient humid air and water conditions by alleviating internal stress and preventing generation of micro-cracks and partial ruptures in wear tracks [13–16]. Moreover, other explanations for that effect have been offered, including the formation of SiO_2 at the frictional interface and an increase in sp^3 hybridization resulting in a less graphitic carbon [17–20]. Thus, the Si would be a good candidate as a doping additional element in the carbon-based coatings.

It is known that the grain boundary sliding was facilitated by increasing the intergrain separation coupled with random orientation, and thus, it can improve the toughness of nanocomposite coating. Because high-angle grain boundaries could minimize incoherent strain and facilitate many nanocrystalline grains to slide in the a-C matrix, it

could release strain and obtain high toughness of coating [21–23]. Another way was reported that imbedding soft and ductile metallic nanocrystalline phase in the hard a-C matrix effectively improved toughness and released internal stress, i.e., aluminum, copper, or silver was incorporated which prevented the formation of stable bonds between the nanocrystallite and the a-C matrix. These would facilitate the grain–matrix interface sliding so as to improve the coating's toughness and release internal stress [24–28]. Of course, incorporation of such metallic element would inevitably cost some hardness of coatings. Besides, such soft metallic Al incorporated in the coating would create a situation where it was more favorable to form graphite in the contact area induced by the elevated temperature in the sliding friction, reported by Wilhelmsson et al. [29]. Thus, the Al would be also a good candidate as a doping additional element in the carbon-based coatings, which can reduce residual stress and improve toughness at certain expense of hardness while achieving self-lubricating behaviors.

Recently, the simplex Si-doped carbon-based coatings (such as a-C:H:Si and a-C:Si) have been widely investigated including microstructure, mechanical, and tribological properties [16, 30, 31]. However, the combination of Si and Al-dopings in carbon-based coatings was scarcely reported. In this study, a mode of duplex-doping was conceived to fabricate the a-C:Si:Al carbon-based coating by the incorporation of Si and Al. In this letter, we mainly focused on the comparative investigations on microstructure, mechanical properties, and tribological moisture sensitivity of as-fabricated a-C:Si and a-C:Si:Al coatings. It was found that the a-C:Si:Al carbon-based coating could possess low residual stress, moderately high hardness, good toughness, and controlled tribological moisture sensitivity coupled with low friction coefficient and high wear resistance under different relative humidity conditions, indicating a great potential for engineering applications.

2 Experimental

2.1 Coatings Preparation

The a-C:Si and a-C:Si:Al carbon-based coatings were deposited on silicon p(100) wafers and stainless steel substrates using magnetron sputtering of Si, Al, and graphite (C) targets of 99.99, 99.99, and 99.80% purity in an argon gas atmosphere. Before deposition, the Si wafers and stainless substrates were first ultrasonically cleaned in acetone and alcohol for 30 min and then put into the depositing chamber. The base pressure of depositing chamber was pumped down to 1.0×10^{-3} Pa, then the chamber was backfilled with Ar gas of 100 sccm flow rate to 0.8 Pa. The substrates were cleaned using Ar^{+} bombardment for 30 min at a substrate bias voltage of −1,000 V to remove some adhering impurities on substrates. Before the coating deposition, a Si interlayer of about 400 nm thick was deposited by sputtering of Si target (300 W of R.F. power supply, −300 V bias voltage and 50% duty ratio) so as to improve the adhesion of the final coatings to the substrate. Subsequently, the carbon-based coatings were deposited under Ar gas of flow rate of 100 sccm. In the depositing, the pulse power supply was kept with 40 kHz frequency, −300 V bias voltage and 50% duty ratio, the D.C. power density of graphite target was kept constant at 6.5 W/cm^2, and the power density of Si (R.F. power supply) and Al (D.C. power supply) targets was varied for desirable composition. During the whole deposition, there was no extra-heating to the substrates.

2.2 Coatings Characterization

The thickness of a-C:Si and a-C:Si:Al carbon-based coatings was measured using a surface profilometre. X-ray photoelectron spectroscopy (XPS) was carried out on PerkinElmer PHI-5702 multi-functional photoelectron spectrometer with Al Kα radiation to investigate the compositions and chemical states of carbon in the coatings. X-ray diffraction (XRD) with a grazing angles of 1° was performed on D/Max-2400X diffractometer (Rigaku Co., Japan), with Cu Kα radiation being applied for phase identification and qualitative texture characterization. A further investigation on microstructure characterization was performed by high-resolution transmission electron microscope (HRTEM) using JEOL 3010 TEM operated at 300 kV. The cross-sectional morphologies of as-deposited carbon-based coatings were investigated using field emission scanning electron microscopy (FESEM, JSM-6701F). The surface morphology and surface roughness of the coatings were observed on an SPM (Nano IIIa) atomic force microscope (AFM). The nanohardness was measured by a Nanotest600 nanoindenter apparatus (MicroMaterials Ltd.) using a Berkovich diamond tip and the maximum indentation depth being kept at 50 nm to minimize the substrate contribution, and the internal stress were measured by the stress induced bending on an interferometric surface profiler. The curvature radii of the substrate before and after the film deposition were measured by the observation of Newton's rings using an optical interferometer system, and then the internal stress was calculated by the Stoney equation. The scratch test was employed to evaluate the adhesion strength on a scratch tester using a diamond indenter of 400 μm in radius by continuously increasing the normal load by 100 N/min. The load at which the friction force assumed a sharp increase was defined as the critical load (L_C) of the coating and used as a quasi-quantitative

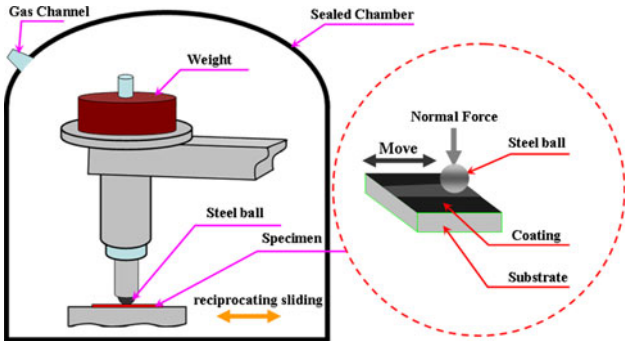

Fig. 1 Schematic diagram of wear test for as-fabricated carbon-based coatings

criterion to evaluate the adhesion strength of the coatings on the substrate.

The tribological moisture sensitivity of as-fabricated carbon-based coatings were evaluated by a ball-on-disk reciprocating sliding tribometer under different relative humidity conditions, while the reference a-C coating was introduced as comparation and the depositing parameters of which were described in Ref. [9]. Friction tests were conducted under the sealed tribometer cover connected with a water bubbler and a dry air supplier. Then, the relative humidity in the testing chamber was precisely controlled about 5, 50, and 90%. Figure 1 shows a schematic diagram of the wear test performed on the coatings. The steel ball with a diameter of 5 mm was used as the counter body, and all frictional tests were performed under a load of 5 N with the amplitude of 5 mm and frequency of 5 Hz. The time of frictional tests was 1 h (18,000 cycles). Subsequently, the wear tracks and wear scars formed on the counterface were characterized by a JSM-5600 SEM, and the corresponding frictional chemical reactions on contact area were analyzed by XPS.

3 Results

3.1 Characterization of As-Fabricated Carbon-Based Coatings

The chemical composition of a-C:Si and a-C:Si:Al carbon-based coatings was calculated from the XPS signals corresponding to C(1s), Si(2p), Al(2p), and O(1s) core levels using standard atomic sensitivity factors of instrument, which was tabulated in Table 1. The composition of a-C:Si coating was determined to about 13.4 at.% Si, 85.1 at.% C, and 1.5 at.% O, and a-C:Si:Al coating was determined to about 9.6 at.% Si, 5.7 at.% Al, 83.5 at.% C, and 1.2 at.% O. It is well known that each element has a unique set of binding energy, and XPS may offer a reliable analysis to the chemical state of the constituent elements. The C1s spectrum in the XPS analysis is mostly used in identifying the chemical state of the amorphous carbon. The fitting of C1s spectra shown in Fig. 2 was performed by decomposing each of them into several components with Gaussian line shapes. The peaks at the binding energies 282.9, 284.2, 285.1, and 286.5 eV corresponded to Si–C bonds in SiC phase, sp^2 carbon bonds, sp^3 carbon bonds, and C–O bonds, respectively. Besides, the peak position of Al2p photoelectron was at about 74.1 eV, which was attributed to partial metallic oxide. Aluminum carbide has a binding energy at 281.5 eV and aluminum oxycarbide has a binding energy at 282.5 eV, both were not seen in the XPS C1s spectra of a-C:Si:Al carbon-based coating. The binding energy of aluminum carbide and aluminum oxycarbide was within the spread of the C1s peak for SiC phase. The peak shapes did not have noticeable difference

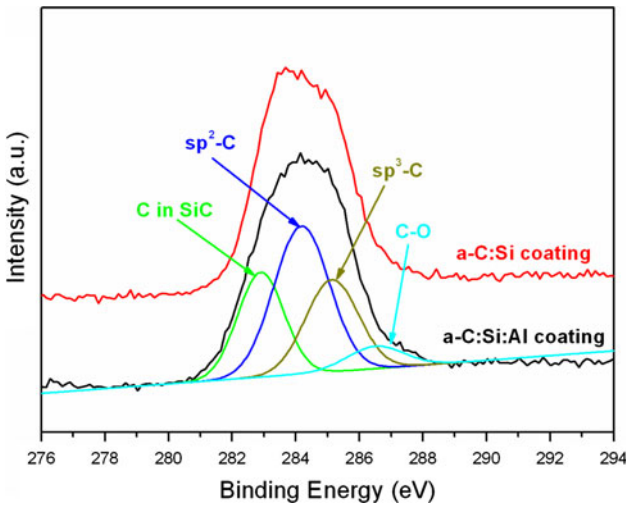

Fig. 2 XPS C1s spectra of a-C:Si and a-C:Si:Al carbon-based coatings

Table 1 Composition and mechanical properties of a-C:Si and a-C:Si:Al carbon-based coatings

Coating	Composition (at.%)				Thickness (μm)	Hardness (GPa)	Elastic modulus (GPa)	*H/E* ratio	Critical load (N)	Residual stress (GPa)
	C	Si	Al	O						
a-C:Si	85.1	13.4	0.0	1.5	2.0	22	241	0.091	13	−1.3
a-C:Si:Al	83.5	9.6	5.7	1.2	2.1	17	189	0.090	19	−0.5

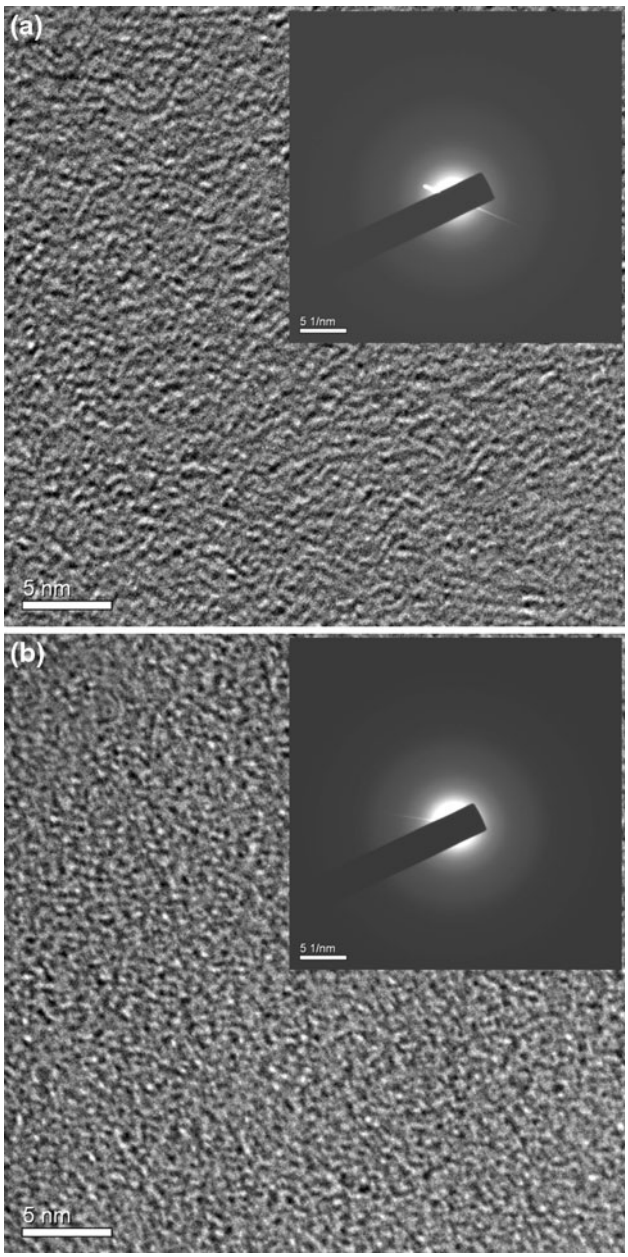

Fig. 3 TEM bright-field images and SAED patterns of as-fabricated coatings: **a** a-C:Si coating, **b** a-C:Si:Al coating

between the two XPS C1s spectra of a-C:Si and a-C:Si:Al carbon-based coatings. Therefore, it was believed that aluminum did not form bonds with carbon, and it existed in the form of the solid solution because of Al belonging to weak-carbide-forming (WCF) metals like Cu, Ag, etc. These were consistent with other researchers' results [29, 32, 33]. Figure 3 shows the HRTEM bright-field images and selected area electron diffraction (SAED) patterns of as-fabricated coatings. HRTEM images revealed that both a-C:Si and a-C:Si:Al carbon-based coatings possessed typical amorphous structure, and the SAED patterns further proved this amorphous structure. It can be found that the Si formed hard SiC phase, though it did not form the nanocrystalline SiC grains in the as-fabricated carbon-based coatings. As a result, the SiC phase and Al all went into the a-C matrix so that both of as-fabricated carbon-based coatings were dominated by the typical amorphous structure.

The surface and cross-sectional morphologies of as-fabricated a-C:Si and a-C:Si:Al carbon-based coatings were observed using FESEM which were exhibited in Fig. 4. As can be seen that a-C:Si carbon-based coating mainly exhibited textured and columnar microstructure, and its thickness was about 2.0 μm. In contrast, a-C:Si:Al coating exhibited more homogeneous and dense microstructure, and its thickness was about 2.1 μm. Besides, the surface morphologies of as-fabricated carbon-based coatings were characterized by AFM, and the two and three-dimensional AFM surface morphologies were shown in Fig. 5. It can be seen that the effect of Al-doping on the surface roughness and feature was apparent. The surface of the coating fabricated with no Al-doping was relatively rough, while the coating fabricated with Al-doping exhibited relatively smooth and uniform. The corresponding root mean square (RMS) roughness of a-C:Si and a-C:Si:Al carbon-based coatings were about 1.2 and 0.9 nm, respectively.

3.2 Mechanical Properties of As-Fabricated Carbon-Based Coatings

The mechanical properties of a-C:Si and a-C:Si:Al carbon-based coatings were systemically investigated. The main results including the hardness (H), elastic modulus (E), H/E ratio, critical load (L_c), and residual stress (σ) were tabulated in Table 1. The value of hardness of a-C:Si and a-C:Si:Al coatings were $\sim$22 and $\sim$17 GPa while the corresponding value of Young's modulus were $\sim$241 and $\sim$189 GPa, respectively. It can be seen that Al co-doping obviously decreased the hardness and Young's modulus of as-fabricated coating. However, the value of H/E ratio of carbon-based coatings nearly occupied the same (about 0.09). Besides, the residual stress values of the two carbon-based coatings were calculated by applying the Stoney equation. The compressive stress of -1.3 and -0.5 GPa corresponded to a-C:Si and a-C:Si:Al coatings, respectively. It was noticeable that the internal stress of carbon-based coating was decreased drastically by co-introduction of Al. For amorphous carbon-based coating of nearly 2.1 μm in thickness, -0.5 GPa of internal stress was very low compared with those hard coatings such as TiC, WC, and TiN which could easily give rise to several GPa [34–36]. The scratch tester was carried out to evaluate the adhesive strength of as-fabricated carbon-based coatings. As can be seen in Table 1, the Al co-doping increased the

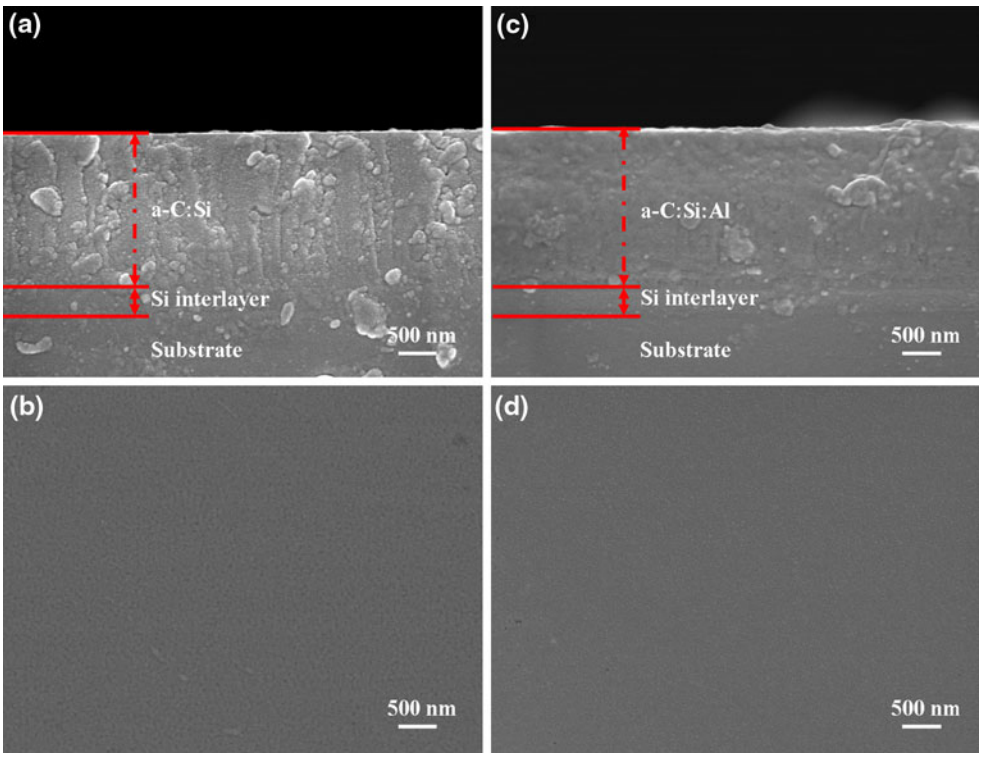

Fig. 4 Cross-sectional and surface images of as-fabricated coatings: **a**, **b** for a-C:Si coating; **c**, **d** for a-C:Si:Al coating

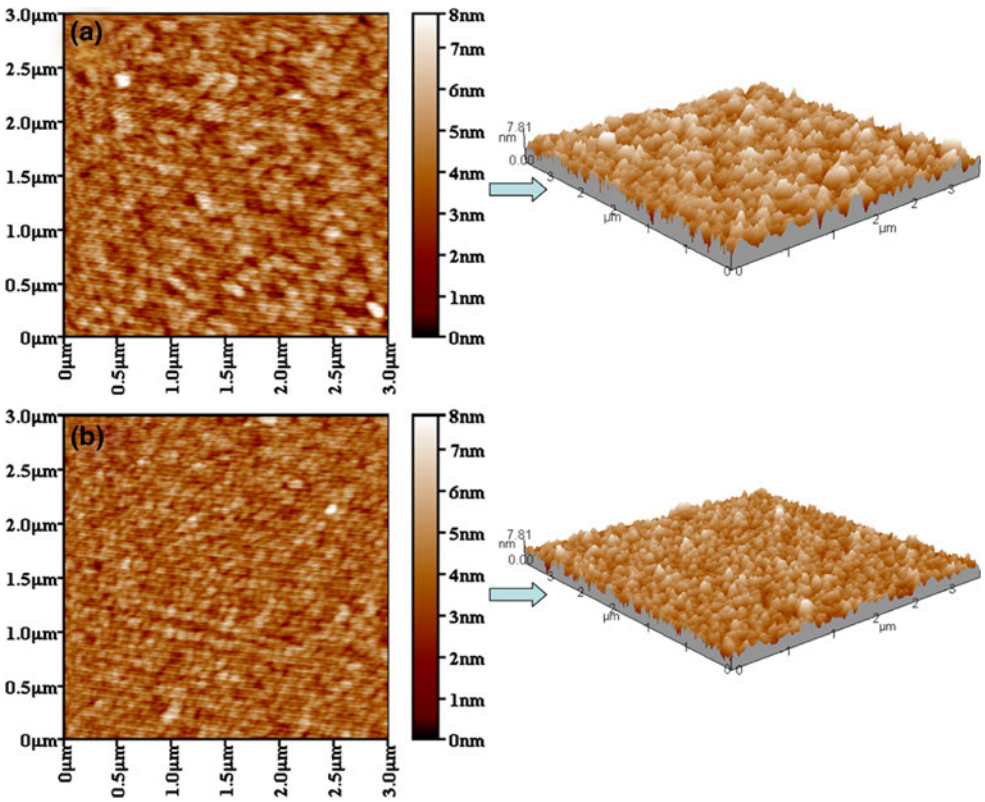

Fig. 5 Two and three-dimensional AFM surface morphologies: **a** a-C:Si coating, **b** a-C:Si:Al coating

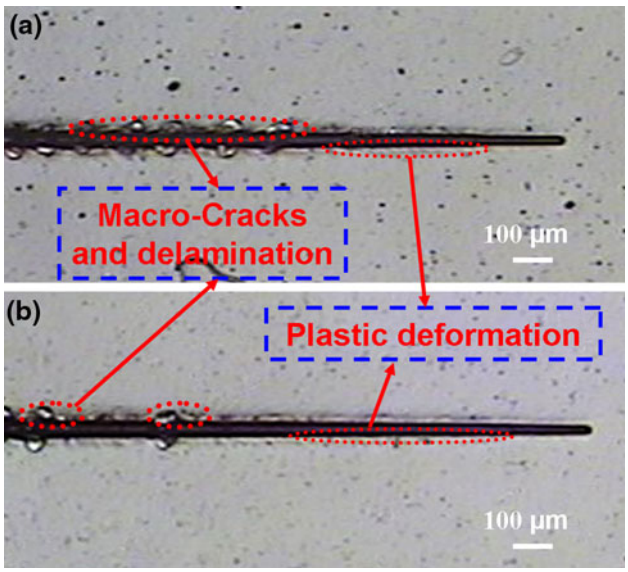

Fig. 6 Optical mages of scratch tracks: **a** a-C:Si coating, **b** a-C:Si:Al coating

critical load to 19 N compared to that of 13 N of a-C:Si coating. Figure 6 shows the optical images of scratch tracks of as-fabricated carbon-based coatings. The a-C:Si coating presented many cracks and abruptly localized delamination of severely brittle characteristic while the a-C:Si:Al coating mainly presented plastic deformation and just few cracks.

By the co-introduction of Al in a-C:Si coating, the magnitude of internal stress was drastically diminished while the relatively high hardness was maintained as well as the adhesive strength was improved. These indicated that a-C:Si:Al carbon-based coating could achieve superior combining of mechanical properties.

3.3 Tribological Behaviors Under Different Relative Humidity Conditions

Figure 7 shows the evolution of the friction coefficient versus sliding time for a-C (a reference hydrogen-free amorphous carbon coating), a-C:Si, and a-C:Si:Al coatings under different relative humidity conditions. For reference a-C coating, the friction coefficient ($\Delta_{(Coeff)} \approx 0.30$) had drastically increased as the relative humidity changed from R.H. 5% to R.H. 90%, indicating that the a-C coating had strong tribological moisture sensitivity. However, the increase of friction coefficient ($\Delta_{(Coeff)} \approx 0.095$) became relatively mild with the relative humidity for a-C:Si coating, indicating that a-C:Si coating had an improved tribological moisture sensitivity compared with the reference hydrogen-free amorphous carbon coating. Furthermore, for a-C:Si:Al coating, the friction coefficient ($\Delta_{(Coeff)} \approx 0.069$) had less

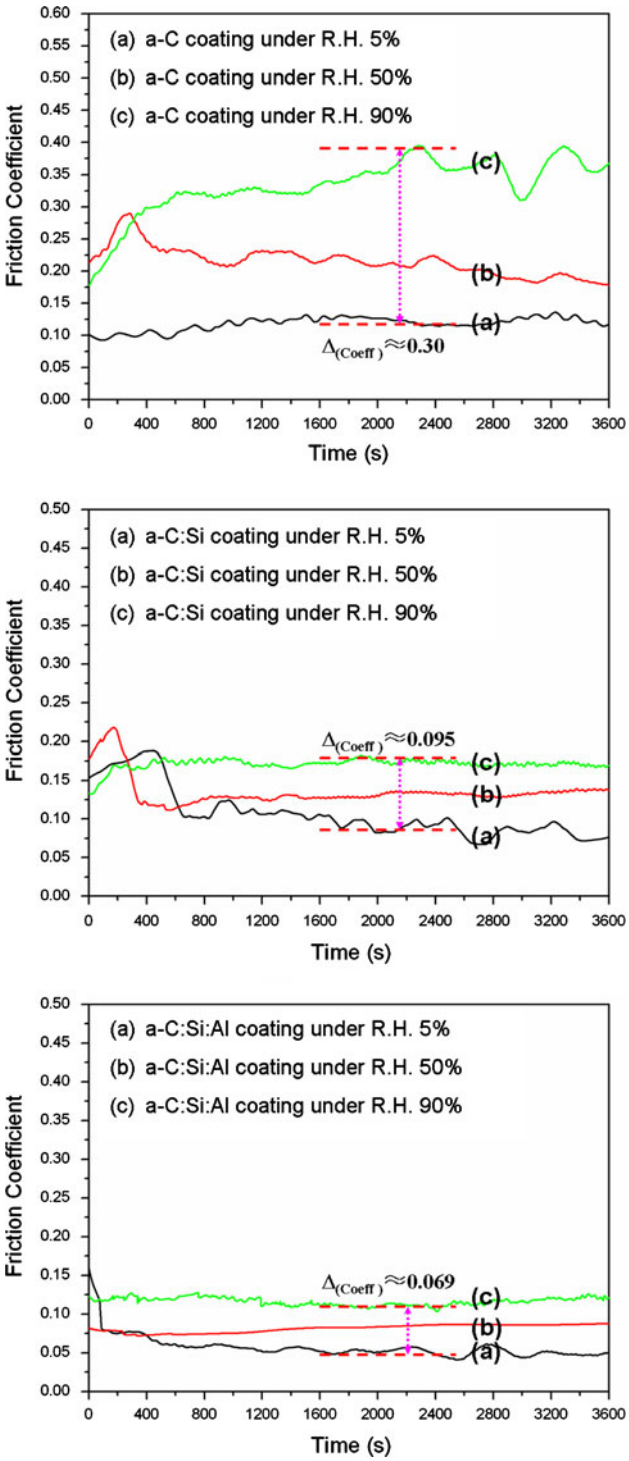

Fig. 7 Friction coefficient versus sliding time for as-fabricated coatings under different relative humidities

increase as the relative humidity changed from R.H. 5% to R.H. 90%. As shown above, the a-C:Si:Al coating exhibited the lowest tribological moisture sensitivity. At the end of each frictional experiment, the wear rate was assessed by taking a profile of the wear track at three different points around the track. The wear data was collated in Fig. 8. It can

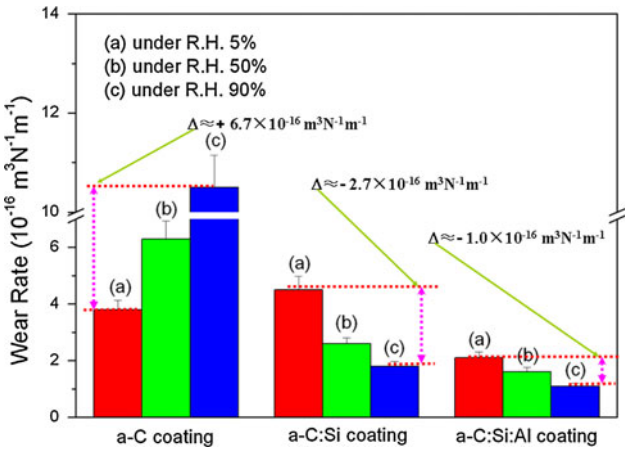

Fig. 8 Wear rate of as-fabricated coatings under different relative humidities

be seen that the wear rate of a-C coating showed a sharp increase as the relative humidity changed from R.H. 5% to R.H. 90%. However, the wear rate of Si-introduced carbon-coatings has been inverted as the relative humidity was increased. The wear rate of a-C:Si and a-C:Si:Al coatings showed a gradual decrease when the relative humidity changed from R.H. 5% to R.H. 90%. Comparing the friction and wear behaviors of the three kinds of carbon-based coatings, the a-C:Si:Al coating clearly presented the best tribological performances under different relative humidities.

Subsequently, the wear tracks and wear scars on counterface were characterized by SEM. Figure 9 shows the SEM images of wear tracks of carbon-based coatings under different relative humidity conditions. For a-C coating, the wear track presented slight wear and rather smooth surface under the R.H. 5% condition while the wear tracks exhibited severe wear and damaged regions under the R.H. 50% and R.H. 90% conditions. However, the wear characteristic was inverted for the Si-introduced carbon-based coatings. For a-C:Si and a-C:Si:Al coating, the wear mechanism was mainly characterized by mild polishing wear. Obviously, the depth of wear tracks became shallower when the relative humidity changed from R.H. 5% to R.H. 90%. Figure 10 shows the SEM images of wear scars on counterface under different relative humidity conditions. For a-C coating, wear scars enlarged and wear debris increased on the edge of contact zone when the relative humidity changed from R.H. 5% to R.H. 90%. For as-fabricated a-C:Si coating, some thick transferred film accumulated on the counterface under the R.H. 5% condition while the transferred film was not observed under the

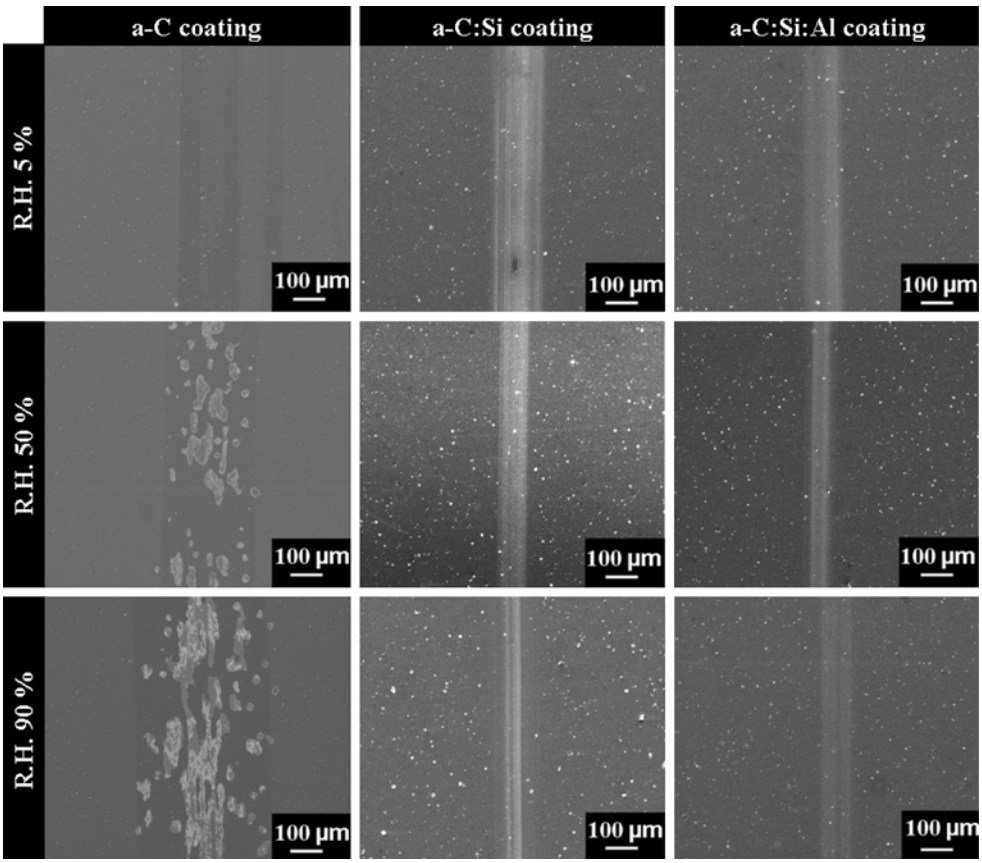

Fig. 9 SEM images of wear tracks of as-fabricated coatings under different relative humidities

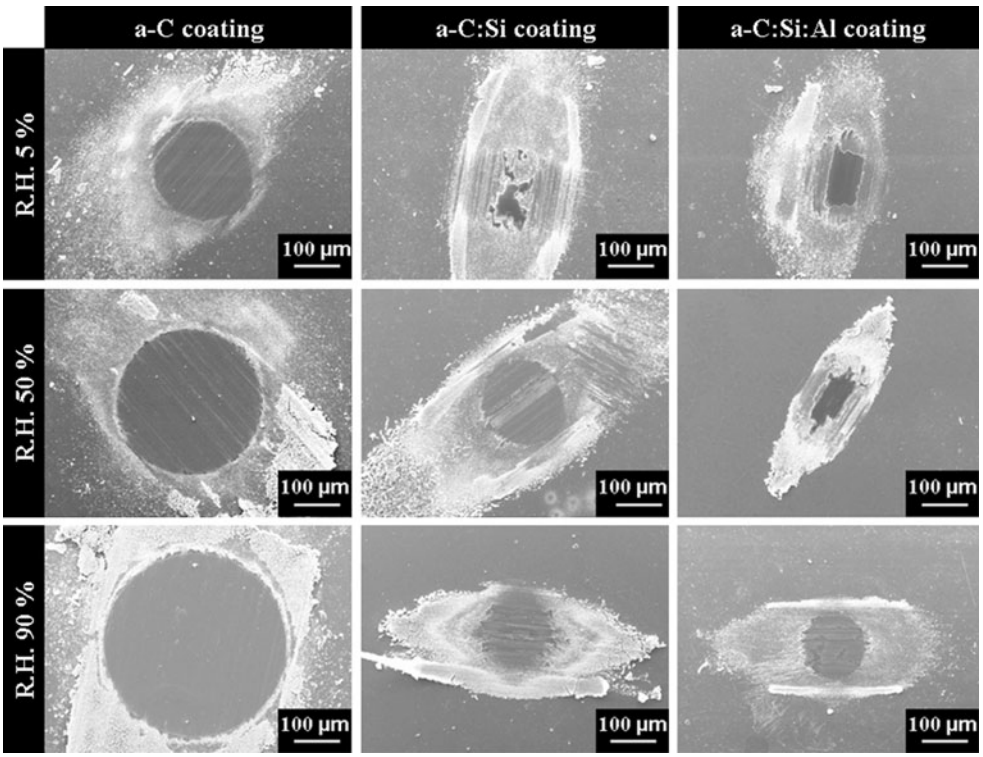

Fig. 10 SEM images of wear scars of as-fabricated coatings under different relative humidities

R.H. 50% and R.H. 90% conditions. The similar general trend was presented on the counterface for a-C:Si:Al coating, while its striking characteristic was more continuously compacted transferred film formed on the counterface under the R.H. 5% and R.H. 50% conditions. Besides, wear tracks for as-fabricated a-C:Si and a-C:Si:Al coatings under different relative humidity conditions were analyzed by XPS as shown in Fig. 11. The peaks near 100.3, 101.3, and 102.3 eV corresponded to SiC, SiO_xC_y, and SiO_x, respectively. As the relative humidity increased, an apparent shift of Si2p peak from 100.3 to 102.3 eV was observed, indicating that some SiC was converted to SiO_x during the sliding friction. Thus, it can be speculated that the colloidal silica (or $SiO_x(OH)_y$) was produced by the tribochemical reaction of Si or SiC with H_2O molecule [16, 17].

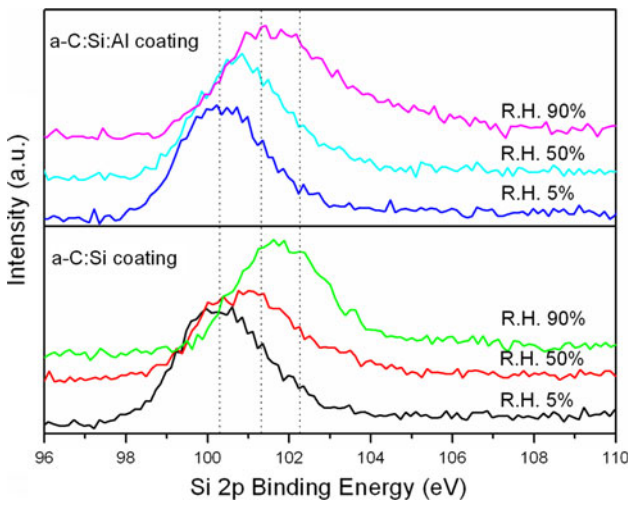

Fig. 11 XPS Si2p spectra of wear tracks of as-fabricated coatings under different relative humidities

4 Discussion

The a-C:Si and a-C:Si:Al carbon-based coatings were successfully fabricated on stainless steel and silicon wafer substrates via magnetron sputtering Si, Al, and graphite (C). XPS revealed that the Si existed in the form of SiC phase because of its strong bond with C, while the Al did not form stable carbide because of its weak bond with C. However, TEM results revealed that the SiC phase did not form the nanocrystalline SiC grains in the as-fabricated carbon-based coatings. The SiC phase and the Al-doping element were all dissolved into the a-C matrix, resulting in both of as-fabricated carbon-based coatings were dominated by the typical amorphous structure. The co-doping of metallic Al strongly affected the mechanical properties of as-fabricated carbon-based coating. References [25, 27] reported that the doping of self-softer metallic Al, like Cu and Ag, can drastically relax the internal stress and

enhance the toughness of carbon-based coatings while at certain expense of hardness. Moreover, the co-introduction of Ti and Al in carbon-based coatings were proposed by researchers, those coatings possessed good mechanical properties [26, 32]. In this study, the results also proved that the magnitude of internal stress could be drastically diminished by the co-introduction of Al in the a-C:Si coating while the relatively high hardness was maintained as well as the adhesive strength was improved. One striking difference between the two carbon-based coatings was that more macro-cracks and delamination were observed in the scratch track of a-C:Si coating, indicating that the a-C:Si coating displayed more brittle characteristic compared with a-C:Si:Al coating. As a result, the a-C:Si:Al carbon-based coating possessed superior combining mechanical properties, which would have great potential for engineering applications.

The effect of atmospheric humidity appeared clearly in friction and wear of the three types of carbon-based coatings. The experimental results revealed that a-C (a reference hydrogen-free amorphous carbon coating) coating possessed strong tribological moisture sensitivity shown in Fig. 7, while coating wear in low relative humidity invariably exceeded that in high relative humidity. This dependence of the friction on relative humidity was similar to that in the case of amorphous carbon films obtained by other researchers [37, 38]. For the engineering applications, a coating capability of providing a low, predictable, and stable friction coefficient across a wide range of relative humidity is of great important in many sectors. Thus, the use of various additive atoms has been proposed to control the tribological moisture sensitivity. In this study, the as-fabricated a-C:Si and a-C:Si:Al presented an apparent improvement of tribological moisture sensitivity. It is well known that the formation of transferred materials from carbon-based coating plays an important role in the reduction of the friction coefficient. As seen in Fig. 10, for as-fabricated a-C:Si coating, some thick transferred film accumulated on the counterface under the R.H. 5% condition while the transferred film was not observed under the R.H. 50% and R.H. 90% conditions. The similar general trend was presented on the counterface for a-C:Si:Al coating, while the striking characteristic was the more continuously compacted transferred film formed on the counterface under the R.H. 5% and R.H. 50% conditions. Gangopadhyay et al. [20] reported that materials transferred on counterface from the carbon-based coating existed in dry air but existed only negligibly on the frictional counterface in wet air, which resembled the present experimental results shown in Fig. 10. Wilhelmsson et al. [29] suggested that the soft metallic Al incorporated in the coating can create a situation where it was more favorable to form graphite in the contact area under dry friction. These speculated that the WCF metallic Al incorporated in a-C:Si carbon-based coating has a great potential to favor an increased segregation of carbon at elevated temperatures induced by sliding friction under low relative humidity. Therefore, the compactly transferred graphitized film on the counterface was easily formed, and this was mainly responsible for the low friction coefficient and wear rate of the a-C:Si:Al coating under low relative humidity. In addition, XPS results of wear tracks for the as-fabricated a-C:Si and a-C:Si:Al coatings under different relative humidities, shown in Fig. 11, revealed an apparent shift of Si2p peak from 100.3 to 102.3 eV, indicating that some SiC was converted to SiO_x during the sliding friction. Hence, superior tribological performances of the as-fabricated a-C:Si and a-C:Si:Al coatings should be attributed to the formation of low shear strength colloidal silica (or $SiO_x(OH)_y$) tribofilm by the tribochemical reaction of Si or SiC with H_2O molecule on contact area under high relative humidity conditions [13, 16, 17]. Moreover, a-C:Si:Al coating presented better tribological performances compared with a-C:Si under high relative humidity becauseof its good combining mechanical properties.

It is known that, the elastic strain to failure, which is related to the *H/E* ratio, is a more suitable parameter for predicting wear resistance [39]: the higher the *H/E* ratio, the higher the resistance to wear of coatings. The *H/E* ratios of the as-fabricated a-C:Si and a-C:Si:Al coatings were very close (about 0.09), indicating that these two carbon-based coatings should have similar wear resistances under the same relative humidity condition. However, the wear results clearly contradicted with the above theory. As discussed above, the a-C:Si:Al carbon-based coating could achieve an excellent self-lubricating behavior under different relative humidities, which might be the main reason for this discrimination of wear resistance. As a result, although the *H/E* ratio of a-C:Si and a-C:Si:Al carbon-based coating stayed almost a constant value, the low shear strength tribofilms on contact zone combining with superior mechanical properties made the a-C:Si:Al carbon-based coating achieve superior tribological performances under different relative humidities.

5 Conclusions

The a-C:Si and a-C:Si:Al carbon-based coatings were comparatively investigated on microstructure, mechanical properties, and tribological moisture sensitivity. The most important results were summarized as follows:

(1) The Si and Al were uniformly dispersed in a-C matrix, and both of as-fabricated a-C:Si and a-C:Si:Al carbon-based coatings were dominated by typical

amorphous structure. The a-C:Si:Al coating exhibited more homogeneous and dense structure as well as relatively smooth surface because of the Al co-doping element compared with a-C:Si coating.

(2) As the WCF Al was co-doped in the as-fabricated carbon-based coating, the magnitude of internal stress was drastically diminished, the adhesive strength was improved as well as the moderately high hardness was maintained.

(3) The a-C:Si:Al carbon-based coating presented superior low tribological moisture sensitivity. The significant improvement in tribological performances of a-C:Si:Al carbon-based coating was mainly attributed to the superior mechanical properties and the formation of continuously compacted graphitized tribofilm under low relative humidity condition as well as low shear strength colloidal silica tribofilm under high relative humidity condition.

(4) The good balance between the hardness and toughness, low internal stress and controlled tribological moisture sensitivity of a-C:Si:Al coating make it a good candidate as solid lubricating coating in engineering applications.

Acknowledgments The authors gratefully acknowledge the financial support from the National Natural Science Foundation of China (Grant No. 50905178) and the National 973 Program of China (Grant No. 2011CB706603).

References

1. Grill, A.: Tribology of diamondlike carbon and related materials: an updated review. Surf. Coat. Technol. **94–95**, 507–513 (1997)
2. Casiraghi, C., Robertson, J., Ferrari, A.C.: Diamond-like carbon for data and beer storage. Mater. Today **10**, 42–51 (2007)
3. Chen, L.Y., Hong, F.C.N.: Diamond-like carbon nanocomposite films. Appl. Phys. Lett. **82**, 3526–3528 (2003)
4. Kalin, M., Vižintin, J.: The tribological performance of DLC-coated gears lubricated with biodegradable oil in various pinion/gear material combinations. Wear **259**, 1270–1280 (2005)
5. Hauert, R.: A review of modified DLC coatings for biological applications. Diam. Relat. Mater. **12**, 583–589 (2003)
6. Ye, J., Okamoto, Y., Yasuda, Y.: Direct insight into near-frictionless behavior displayed by diamond-like carbon coatings in lubricants. Tribol. Lett. **29**, 53–56 (2008)
7. Zhou, F., Adachi, K., Kato, K.: Comparisons of tribological property of a-C, a-CN_x and BCN coatings sliding against SiC balls in water. Surf. Coat. Technol. **200**, 4471–4478 (2006)
8. Corbella, C., Vives, M., Pinyol, A., Bertran, E., Canal, C., Poloa, M.C., Andujar, J.L.: Preparation of metal (W, Mo, Nb, Ti) containing a-C:H films by reactive magnetron sputtering. Surf. Coat. Technol. **177–178**, 409–414 (2004)
9. Wang, Y., Wang, L., Wang, S.C., Zhang, G., Wood, R., Xue, Q.: Nanocomposite microstructure and environment self-adapted tribological properties of highly hard graphite-like film. Tribol. Lett. **40**, 301–310 (2010)
10. Ohana, T., Suzuki, M., Nakamura, T., Tanaka, A., Koga, Y.: Low-friction behaviour of diamond-like carbon films in a water environment. Diam. Relat. Mater. **15**, 962–966 (2006)
11. Li, H., Xu, T., Wang, C., Chen, J., Zhou, H., Liu, H.: Humidity dependence on the friction and wear behavior of diamond-like carbon film in air and nitrogen environments. Diam. Relat. Mater. **15**, 1585–1592 (2006)
12. Wang, C.Z., Ho, K.M.: Structural trend in amorphous carbon. Phys. Rev. B **50**, 12429–12436 (1993)
13. Choi, J., Kawaguchi, M., Kato, T., Ikeyama, M.: Deposition of Si-DLC film and its microstructural, tribological and corrosion properties. Microsyst. Technol. **13**, 1353–1358 (2007)
14. Donnet, C.: Recent progress on the tribology of doped diamond-like and carbon alloy coatings: a review. Surf. Coat. Technol. **100–101**, 180–186 (1998)
15. Kim, S.G., Kim, S.W., Saito, N., Takai, O.: Effect of increasing hardness on Si-containing diamond-like carbon film during tribotest. Diam. Relat. Mater. **19**, 1017–1020 (2010)
16. Gilmore, R., Hauert, R.: Comparative study of the tribological moisture sensitivity of Si-free and Si-containing diamond-like carbon films. Surf. Coat. Technol. **133–134**, 437–442 (2000)
17. Zhao, F., Li, H., Ji, L., Mo, Y., Quan, W., Du, W., Zhou, H., Chen, J.: Superlow friction behavior of Si-doped hydrogenated amorphous carbon film in water environment. Surf. Coat. Technol. **203**, 981–985 (2009)
18. Gilmore, R., Hauert, R.: Control of the tribological moisture sensitivity of diamond-like carbon films by alloying with F, Ti or Si. Thin Solid Films **398–399**, 199–204 (2001)
19. Oguri, K., Arai, T.: Tribological properties and characterization of diamond-like carbon coatings with silicon prepared by plasma-assisted chemical vapour deposition. Surf. Coat. Technol. **47**, 710–721 (1991)
20. Gangopadhyay, A.K., Willermet, P.A., Tamor, M.A., Vassell, W.C.: Amorphous hydrogenated carbon films for tribological applications. I. Development of moisture insensitive films having reduced compressive stress. Tribol. Int. **30**, 9–18 (1997)
21. Voevodin, A.A., O'Neill, J.P., Zabinski, J.S.: Tribological performance and tribochemistry of nanocrystalline WC/amorphous diamond-like carbon composites. Thin Solid Films **342**, 194–200 (1999)
22. Voevodin, A.A., Zabinski, J.S.: Supertough wear-resistant coatings with 'chameleon' surface adaptation. Thin Solid Films **370**, 223–231 (2000)
23. Pei, Y.T., Galvan, D., De Hosson, J.T.M.: Nanostructure and properties of TiC/a-C:H composite coatings. Acta Mater. **53**, 4505–4521 (2005)
24. Dub, S., Pauleau, Y., Thiery, F.: Mechanical properties of nanostructured copper-hydrogenated amorphous carbon composite films studied by nanoindentation. Surf. Coat. Technol. **180–181**, 551–555 (2004)
25. Pauleau, Y., Thiery, F., Latrasse, L., Dub, S.: Characteristics of copper/carbon and nickel/carbon composite films produced by microwave plasma-assisted deposition techniques from argon-methane gas mixtures. Surf. Coat. Technol. **188–189**, 484–488 (2004)
26. Tay, B.K., Cheng, Y.H., Ding, X.Z., Lau, S.P., Shi, X., You, G.F., Sheeja, D.: Hard carbon nanocomposite films with low stress. Diam. Relat. Mater. **10**, 1082–1087 (2001)
27. Zhang, G., Yan, P., Wang, P., Chen, Y., Zhang, J.: The preparation and mechanical properties of Al-containing a-C:H thin films. J. Phys. D Appl. Phys. **40**, 6748–6753 (2007)
28. Lungu, C.P.: Nanostructure influence on DLC-Ag tribological coatings. Surf. Coat. Technol. **200**, 198–202 (2005)
29. Wilhelmsson, O., Råsander, M., Carlsson, M., Lewin, E., Sanyal, B., Wiklund, U., Eriksson, O., Jansson, U.: Design of nanocomposite low-friction coatings. Adv. Funct. Mater. **17**, 1611–1616 (2007)

30. Veres, M., Koos, T.M., Toth, S., Fule, M., Pocsik, I., Toth, A., Mohai, M., Bertoti, I.: Characterisation of a-C:H and oxygen-containing Si:C:H films by Raman spectroscopy and XPS. Diam. Relat. Mater. **14**, 1051–1056 (2005)
31. Kulikovsky, V., Boháč, P., Zemek, J., Vorlíček, V., Kurdyumov, A., Jastrabík, L.: Hardness of nanocomposite a-C:Si films deposited by magnetron sputtering. Diam. Relat. Mater. **16**, 167–173 (2007)
32. Zhang, S., Bui, X.L., Fu, Y.: Magnetron-sputtered nc-TiC/a-C(Al) tough nanocomposite coatings. Thin Solid Films **467**, 261–266 (2004)
33. Pang, X., Shi, L., Wang, P., Zhang, G., Liu, W.: Influences of bias voltage on mechanical and tribological properties of Ti–Al–C films synthesized by magnetron sputtering. Surf. Coat. Technol. **203**, 1537–1543 (2009)
34. Tang, J., Zabinski, J., Bultman, J.: TiC coatings prepared by pulsed laser deposition and magnetron sputtering. Surf. Coat. Technol. **91**, 69–73 (1997)
35. Wänstrand, O., Larsson, M., Hedenqvist, P.: Mechanical and tribological evaluation of PVD WC/C coatings. Surf. Coat. Technol. **111**, 247–254 (1999)
36. Perry, A.J., Valvoda, V., Rafaja, D.: X-ray residual stress measurement in TiN, ZrN and HfN films using the Seemann-Bohlin method. Thin Solid Films **214**, 169–174 (1992)
37. Kim, D.S., Fischer, T.E., Gallois, B.: The effect of oxygen and humidity on friction and wear of diamond-like carbon films. Surf. Coat. Technol. **49**, 537–542 (1991)
38. Yoon, E.S., Kong, H., Lee, K.R.: Tribological behavior of sliding diamond-like carbon films under various environments. Wear **217**, 262–270 (1998)
39. Leyland, A., Matthews, A.: On the significance of the *H/E* ratio in wear control: a nanocomposite coating approach to optimised tribological behaviour. Wear **246**, 1–11 (2000)